

Research Article

Travelling-Wave, Quasi-Periodic, and Persistent Longulent States of the Galerkin-Regularized Hydrodynamic-Type Systems

Jian-Zhou Zhu¹

1. Su-Cheng Centre for Fundamental and Interdisciplinary Sciences, China

Travelling-wave, quasi-periodic and “longulent” states of the Galerkin-regularized systems preserving finite Fourier modes are exposed. The longulent states are characterized by solitonic structures, called “longons”, accompanied by disordered components, which is associated to whiskered tori with the a-posteriori Kolmogorov-Arnold-Moser (KAM) theorem. On-torus invariants are introduced for constructing the KAM tori, towards a potential theory of pseudo-integrability in the sense of specifying precisely the corresponding whiskered tori. Persistence of the longulent states with respect to certain dispersion and dissipation (fine matched by a particularly designed driving model) perturbations are also suggested with numerical results.

1. Introduction

The Galerkin truncation/regularization (Gr) preserving finite Fourier modes regularizes the otherwise rough/singular compactons, peakons^{[1][2][3][4][5]}, and the more familiar Burgers-Hopf (BH) shocks, resembling yet differing from the linearly dispersive Korteweg-de Vries (KdV) regularization. Such or similar truncations are widely used in analysis, computation, and effective field theories.

No travelling-wave or quasi-periodic solutions, or, invariant tori (associated to solitonic structures) can be found in the studies over around 80 years on such conservative Gr-systems some of which being explicitly canonical Hamiltonian (see, e.g., closely relevant Refs.^{[6][7][8][9]} and references therein). So, we should pave the way of such a direction like what have been done in the integrable soliton theory^{[10][11]}. If successful, with also solitonic structures or the corresponding solutions

similar to those quasi- or almost-periodic ones in integrable systems being discovered, then a “pseudo-integrability” theory to bridge the conventional nonintegrability and integrability or some new mathematical results similarly going to a deeper level should be further developed.

This work carries on the above mission, passing the game with surprisingly fruitful results (not harvesting “everything” systematically or completely with full mathematical rigor though). Furthermore, persistence of the invariant tori with respect to dispersive, dissipative and driving perturbations are addressed, with explicit models verified numerically, and the results are related to the fundamental a-posteriori Kolmogorov-Arnold-Moser (KAM) theorem¹ for presumably whiskered tori.

The fundamental results are of broad potential realistic relevance. For example, a remarkable physical application of the torus persistence or chaos control is, among other common problems such as that in celestial mechanics, to construct and sustain magnetic surfaces, a kind of transport barrier^{[12][13]}, in fusion plasmas for which some computer-assisted-proof software package is already available²: we will come back to offer more remarks on this and others (such as fluid turbulence).

Let $v(x, t)$ solve, with x -period 2π and $v_0 = v(x, 0)$,

$$v_t + vv_x = a. \tag{1}$$

As models in plasma and hydrodynamic nonlinear waves, and quantum shocks, among others, $a = 0$, $\mp v_{txx}/9 \mp 2v_x v_{xx}/27 \mp vv_{xxx}/27$, μv_{xxx} , and $\nu(v^2)_{xxx}$ identify, respectively, the BH, compacton/peakon (CP^{[2][11]}), KdV and Rosenau-Hyman^[5] compacton [RH or $K(2, 2)$] equations. In the CP model [reverting to the convenient form $v_t \pm v_{txx} + 3vv_x = \mp 2v_x v_{xx} \mp vv_{xxx}$ with the x -rescaling factor 3 from now on], the upper signs correspond to the compacton, and the lower to the Camassa-Holm (CH) peakon model^[3].

Let us consider the problem in the period $[0, 2\pi)$. We have the Fourier coefficient \hat{v}_k of v , with $\hat{v}_k^2 = -1$ and complex conjugacy (c. c.) $\hat{v}_k^* = \hat{v}_{-k}$ for reality; similarly, $v\partial_x v = \sum_k \hat{b}_k e^{ikx}$. For v_0 well-prepared in $\mathcal{S} = \{k : -K \leq k \leq K\}$ (“Galerkin space” hereafter), we can calculate each extra-Galerkin \hat{b}_m for $K < |m| (\leq 2K)$ from the intra-Galerkin \hat{v}_k s for $k \in \mathcal{S}$. In the BH case, setting \hat{a}_m to be $\hat{g} = \hat{b}_m$ for $m \notin \mathcal{S}$, otherwise 0, results in the Galerkin truncation: for all $m \notin \mathcal{S}$, $\hat{v}_m(t) \equiv 0$ ($t > 0$), thus the Galerkin-regularized BH (GrBH), and GrKdV with the same form; and, similarly, the GrCP, or, GrCH and GrRH systems with their respective .

To be more explicit, we write down the equation for the above GrBH system, with $P_K v(x) := \sum_{|k| \leq K} \hat{v}_k \exp\{i k x\} =: u$, $B := u^2/2$ and $:= B - P_K B$ ^[6],

$$Du/Dt := \partial_t u + \partial_x B = \partial_x u; u_0 = P_K v_0. \quad (2)$$

The Galerkin force $= \partial_x u$, with \hat{v}_k for $K < |m| \leq 2K$, can be excited only when there exists $\hat{u}_k \neq 0$ with $k > K/2$. Such and other Gr-system ones are nonlinear dispersions.

The CP Hamiltonian operator $J_{CP} = -2\pi(\partial_x \pm \partial_x^3)$ in Fourier representation still applies with truncation and is inherited by GrCP, just like $J_{KdV} = -2\pi\partial_x$ ^[14]. The GrBH reduction replaces the Hamiltonian $\mathcal{H}_{BH} = \int_0^{2\pi} \frac{v^3 dx}{12\pi}$ with^[7]

$$\mathcal{H} = \sum_{p,q,k=p+q \in} \frac{\hat{u}_k^* \hat{u}_p \hat{u}_q}{6} = \int_0^{2\pi} \frac{u^3 dx}{12\pi}. \quad (3)$$

$= \mathcal{H}_{BH} - \mathcal{H}$ is called the Galerkin interaction potential. The alternative BH Hamiltonian operator $J'_{BH} := -(u\partial_x + \partial_x u)/3$ involves u and is not transferable to GrBH. Only three GrBH invariants, \mathcal{H} , $\mathcal{E} = \int_0^{2\pi} \frac{u^2 dx}{4\pi}$ and $\mathcal{M} = \hat{u}_0 = \int_0^{2\pi} \frac{u dx}{2\pi}$ are known to survive for general K (“rugged”); similarly for the GrKdV and GrCP situations, with, e.g., $\mathcal{H}_{CP} = \int_0^{2\pi} \frac{v^3 \mp v(\partial_x v)^2}{4\pi} dx$ and, accordingly, \mathcal{M}_{CP} and \mathcal{E}_{CP} , and, their Gr-versions. By Galilean invariance, \mathcal{M} is taken to be zero or truncated in this study, and K is effectively the number of available modes (pairs of conjugate Fourier components) with $2K$ degrees of freedom.

As said, the study starts from the dynamical nature of the truncating force and the possibility of bridging nonintegrability and integrability, by the notion of pseudo-integrability with some similar or modified features or techniques of the latter. We will present travelling-wave and multi-phase solutions and show instabilities lead to states dominated by solitonic structures (that we call “longons”) amidst weaker less-ordered components, the “longulent states” or “longulence”. The mechanism for the associated de-thermalization appears akin to that of integrable systems, beyond the “Hamiltonian effect” concerned earlier^{[7][8]}, which motivates proposing the notion of “pseudo-integrability” with appropriate on-torus or torus-specific but not rugged invariants (used for constructing quasi-periodic solutions). In particular, a-posteriori KAM theorem^[15] is suggested and associated to the longulence whose persistence against particular linear dispersion and dissipation (balanced by a fine-matched driving model) will be demonstrated.

2. Analyses

2.1. Travelling waves and interacting longons

We begin with Gr-system example/special solutions of the travelling-wave form, $u^\#(x, t) = u^\#(\zeta)$ with $\zeta = x - \lambda t$, satisfying

$$\partial_t \hat{u}_k^\# = -\frac{\hat{i}k}{2} \sum_{p,q,p+q=k \in \mathbb{Z}} \hat{u}_p^\# \hat{u}_q^\# = -\hat{i} \lambda k \hat{u}_k^\#. \quad (4)$$

For $\lambda = 0$, immediate examples include those with a single mode in $(K/2, K]$; while, with an arbitrary phase parameter x_0 , $u^\# \propto 2\cos[K(x - x_0)/3] - \cos[K(x - x_0)]$ for $\text{mod}(K, 3) = 0$ are less-trivial ones more of which we will come back to later. With $x_0 = 0$ henceforth, we note that, for instance, $u^\# \propto 2\cos(2x) - \cos(6x)$ also solves Eq. (4) in , besides , without exciting/occupying $|k| = 7$; so, another wavenumber parameter S for the maximal $|k|$ occupied by $u^\#$ is naturally introduced below. For moving waves ($\lambda \neq 0$) occupying L modes equally spaced in $|k|$, with $\text{mod}(S, L) = 0$ and $S \leq K < (L + 1)S/L$, we find, by straightforward calculation with $L = 2$,

$$u^\# = 2\sqrt{2}|\lambda|\cos(S\zeta/2) + 2\lambda\cos(S\zeta). \quad (5)$$

Others similarly follow. For instance, taking $\lambda > 0$, with $\theta = S\zeta$, we have a three-mode-occupation wave,

$$u^\# = \lambda[-2\chi_1\cos(\theta/3) + \chi_2\cos(2\theta/3) - \chi_1\chi_2\cos\theta] \quad (6)$$

where $\chi_1 = \sqrt{\frac{5-\sqrt{5}}{5}}$ and $\chi_2 = \sqrt{5} - 1$.

Accordingly, $\propto S\lambda^2$; for example, corresponding to Eq. (5),

$${}^K g^\# = -(S\lambda^2)[3\sqrt{2}\sin(3\theta/2) + 4\sin(2\theta)]/2. \quad (7)$$

Eq. (5) extends to GrKdV-GrRH waves, with both the ν and μ terms for unification,

$$u^\# = 2\sqrt{\frac{\lambda - \mu S^2}{1 + 2\nu S^2}} \chi \cos \frac{\theta}{2} + \chi \cos \theta \quad (8)$$

with $\chi = (4\lambda - \mu S^2)/(2 + \nu S^2)$; and, for the GrCP model,

$$\frac{u^\#}{\lambda} = \frac{4}{3} \sqrt{\frac{2(1 \mp S^2)}{(4 \mp S^2)}} \cos \frac{\theta}{2} + \frac{2}{3} \cos \theta. \quad (9)$$

The parameters of course should be appropriately taken to have positive values under $\sqrt{\bullet}$ and nonvanishing denominator.

Note that there is already the linearly dispersive regularization of BH in KdV which, however, unlike the odd-order-nonlinearity cases such as the cubically-nonlinear modified KdV (mKdV) or nonlinear Schrödinger (NLS) systems, there is no single-mode or monochromatic (condensate) solution that would be independent of the truncation threshold K ; so, in the situation for the above $u^\#$ being valid, it does not make sense to talk about the convergence to KdV of GrKdV.

$u^\#$ s occupying many $|k|$ s may be obtained numerically or with the help of symbolic-computation softwares; e.g., with $\text{mod}(S, 4) = 0$, approximate η s ($\{\eta_1, \eta_2, \eta_3, \eta_4\}$ s) can be found in the ansatz

$$\frac{u^\#}{2\lambda} \approx \eta_1 \cos \frac{\theta}{4} + \eta_2 \cos \frac{\theta}{2} + \eta_3 \cos \frac{3\theta}{4} + \eta_4 \cos \theta. \quad (10)$$

Specifically, $\eta \approx \eta^c = \{-0.507, 0.450, -0.376, 0.292\}$ correspond to a GrBH case resembling the cnoidal wave, except for weaker wiggles between the strong pulses, which is also the case for Eqs. (8) and (9). [It is relatively easy to find by hand some very specific solutions for S up to 7, and many more general ones can be found with the help of symbolic computation software quickly for such an S .]

Wiggle counts grow with mode numbers, as shown in Fig. 1's top and middle panels, using $K = S$ [always so below: other K s ($< S + S/L$) yield the same scenario, modulo quantitative variances.] Such (time-)periodic $u^\#$ -orbits, together with other quasi-periodic tori to be constructed later, are associated to interacting solitonic structures, i.e., the "longons" to be explained eventually, akin to the x -periodic KdV (multi-)soliton analogue^{[10][11]}.

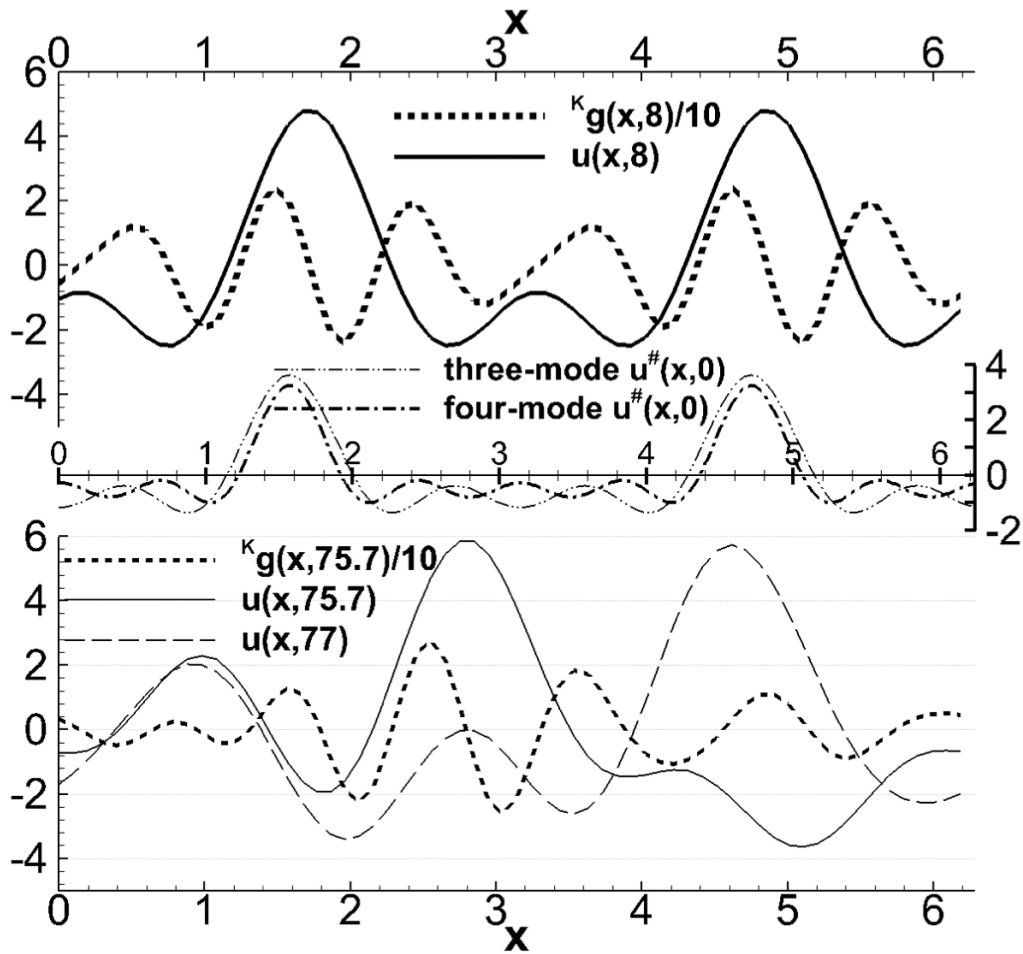


Figure 1. GrBH fields for $K = 4$ and $\lambda = 1$ of the two-active-mode solitary wave, at two regimes (upper and lower frames): $u(x, t)$ at $t = 8$ obeying Eqs. (5) transitioning to an interacting-longon state at $t = 75.7$ [with $u(x, 77)$ added particularly to show varying crest and trough levels]. The middle frame for the three- and four-mode-occupation $u^\#$ s with $\lambda = 1$ at $t = 0$, respectively Eq. (6) for $K = 6$ and Eq. (10) for $K = 8$ with η^e , is inserted to show the similarity and differences. Results of other Gr-systems are of similar fashion and not shown.

Pseudo-spectral computations (discussed later) indicate that, as shown in Fig. 2, for $L \geq 2$ with unoccupied ks in the respective $u_0^\#$, instability eventually transforms the waves into robust states with interacting strong solitonic ‘longons’ amid weaker, less-ordered components of various propagating speeds roughly proportional to the signed strengths, featuring more widely separated crests and troughs whose levels vary slightly: such “longulent” states correspond presumably whiskered tori and, with respect to time, are “pseudo-periodic” in the sense that the weaker components introduce

deviations from strict (quasi-)periodicity. The apparently solitonic longons locally resemble the Mexican hat. This is even clearer in larger- K cases, as exemplified later in Fig. 3. There are waves of other shapes, with various organizations of the strong pulses and weak wiggles indicating some (yet unknown) symmetry in the solutions, which were observed in the developing phases but not in the developed/mature solitonic longons.

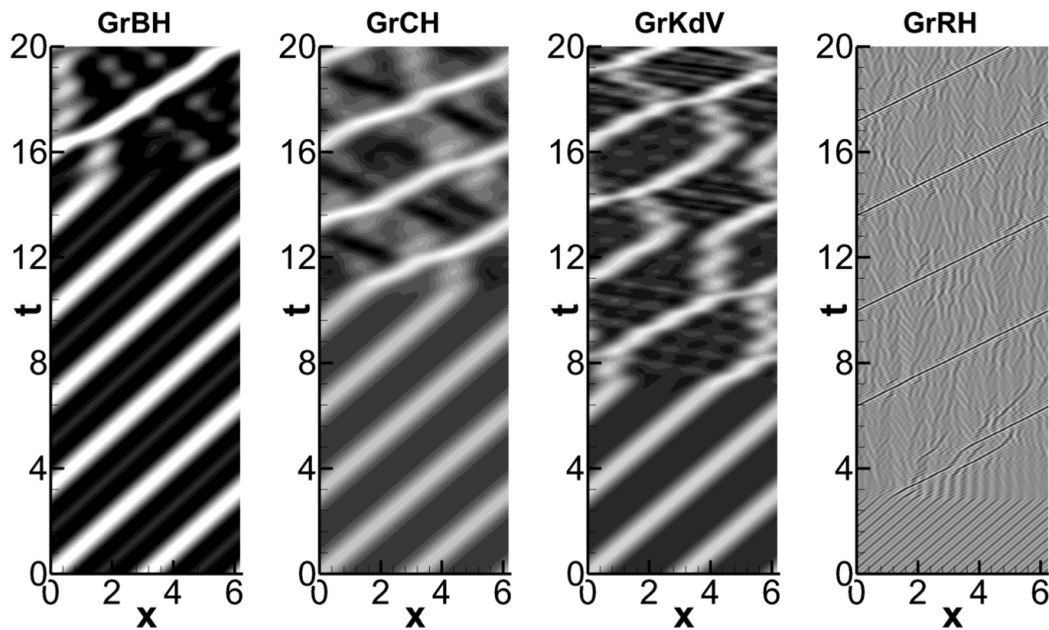


Figure 2. Space-time u -contours of the Gr-systems ($\lambda = 1$): GrBH with $K = 4$, GrCH with $K = 4$ (larger u is brighter as can be read from Fig. 1's top frame; similarly for others), GrKdV with $K = 4$ and $\mu = -0.2$, and, GrRH with $K = 32$ and $\nu = -4$.

Mature longons exhibit a half-wavelength oscillation within each strong(est) pulse, similar to the case of travelling-wave $u^\#$ s. This feature is universal across all Gr-systems studied here, with only minor differences in details such as strengths, as partially shown in Fig. 2. The GrCP compacton branch requires rescaling to mitigate the issue of vanishing denominators, yet its outcomes are similar to those of the peakon branch and hence are not presented here. The “universality” is also in the sense that the major features from such a low K ($= 4$) extend to large K 's (see below), which is further demonstrated by the GrRH case with $K = 32$ where a sharp solitonic ‘dark’ (negative-sign) longon emerges subsequent to the apparent breakdown of the travelling-wave $u^\#$.

The whiskered torus, thus the “longon” carrying the interaction potential, echoes the image of the oriental dragon, i.e., “Long” in Chinese Pinyin for “龙”, the force carrier for various interactions between, say, human and nature, which embodies the transformation between finitude and infinity, upholding order amidst (potential) chaos. We have seen that such tori attract the heteroclinic orbits from nearby approximations starting from which it is possible to establish the a-posteriori KAM theorem^[15], with only minor detailed differences in the proofs for different Gr-systems. We will henceforth focus on the GrBH case for further analysis.

2.2. Gr-continuum on the lattice

Let the periodic lattice coordinate satisfy $x_j = x_{j+N}$, whence $v(x_{j+N}) = v(x_j) =: v_j$ for $j = 0, 1, 2, \dots, N-1$, defining a discrete torus \mathbb{T}_N . The theoretical foundation of the standard (pseudo-)spectral method and the lattice representation of the GrBH continuum lies in replacing \hat{v}_k defined earlier by the discrete Fourier transform (DFT) for $|k| \leq M$ (with $N-1 = 2M$ here), $\hat{\tilde{v}}_k := \sum_{x_j \in \mathbb{T}_N} \frac{v_j}{N} e^{-ikx_j} = \hat{v}_k + \sum_{i \neq 0} \hat{v}_{k+iN}$ (e.g., Ref.^[16]). The aliasing error, represented by the second term, can be mitigated using dealiasing techniques like zero-padding or, alternatively speaking, truncation at $K < N/3$ (“2/3-rule”). Unifying the dealiasing and the Galerkin truncation results in, correspondingly, $\hat{\tilde{u}}_k = \hat{u}_k$ for $u = P_K v$ in the GrBH equation (2), i.e., $\partial_t u_j = -P_K \partial_x u_j^2/2$, so

$$\partial_t u_j = \sum_{p+q=k \in \mathbb{T}_N} \sum_{x_n \in \mathbb{T}_N} \frac{k u_m u_n e^{i(kx_j - px_m - qx_n)}}{2iN^2} \quad (11)$$

where the right-hand side in physical-space variables reveals the GrBH lattice dynamics explicitly.

The pseudo-spectral method computes GrBH in Fourier space, evaluating the nonlinear term in physical space via DFT of $P_K u_j^2$, $\partial_t \hat{u}_k = -\frac{ik}{2} \sum_{j=0}^{N-1} \frac{P_K(u_j^2)}{N} e^{-ikx_j}$, so the computation aligns precisely with the GrBH definition, with only round-off errors and time discretization. Note that even the “spectral-accuracy” errors, for the smooth solutions to classical differential equations do not exist for us.

Since fourth-order Runge-Kutta scheme and its variant (for an approximation below) are used, the numerical results are highly accurate and reliable. Linear analysis (e.g., Lyapunov) of perturbed GrBH solutions (around, say, $u^\#$) indicates generic instability. And, conventional nonlinear analyses, such as orbital instability analysis, must contend with the unconventional. Here, the numerical results potentially provide clues for further establishing relevant analytical insights.

2.3. Hamiltonian extrema and persistence of longlence against a linearly-dispersive perturbation

Notably, the critical set extremizing \mathcal{H} via

$$\delta(\mathcal{H} - \lambda\mathcal{E})/\delta u = 0 \quad (12)$$

corresponds to Eq. (4). Including another multiplier λ_0 for \mathcal{M} , vanishing or not, doesn't matter, as in the KdV finite-gap theory^{[10][11]}. For the large- K GrBH problem, there are in general $= 2[K + \text{sgn}(|\mathcal{M}|)] - 1 - |k|$ triads satisfying $p + q = k$ for each k . If were independent of k , then $\hat{u}_k = c(\lambda)$, a real constant uniform over k would extremize \mathcal{H} . Therefore, for large K , with changing relatively slow with k ,

$$u_0 = [\cos(x) + \cos(2x) + \dots + \cos(Kx)]/\sqrt{K} \quad (13)$$

is an appropriate typical large-Hamiltonian but non-travelling-wave initial data for GrBH.

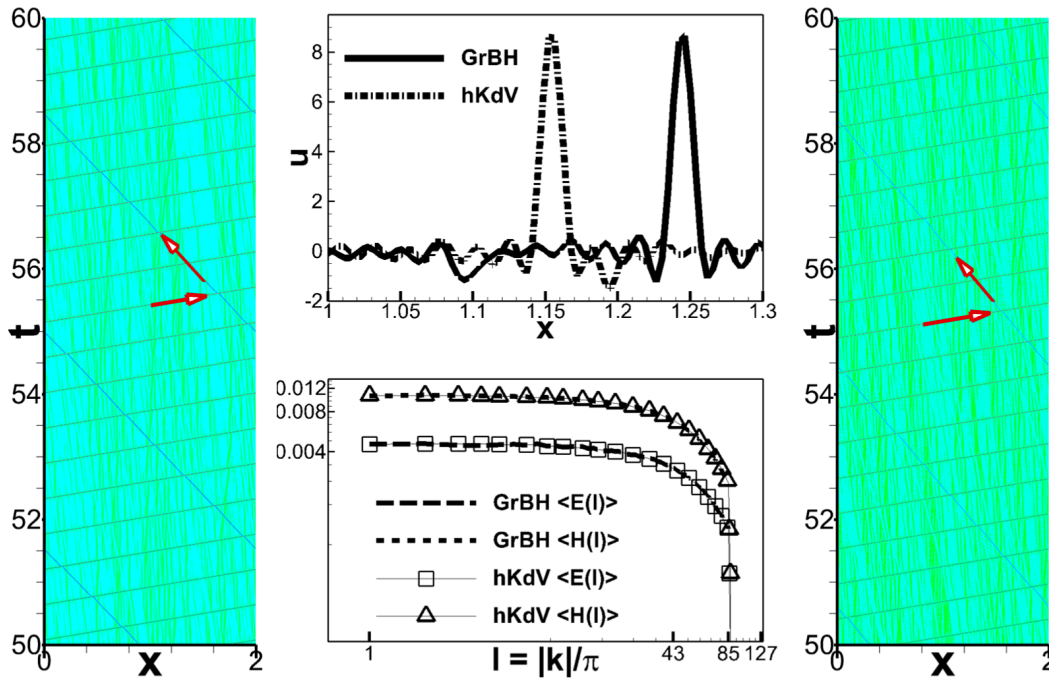


Figure 3. GrBH (left) and hKdV (right) u -contours, u -profile snapshots (middle, upper) of GrBH and hKdV at, respectively, $t = 59.9$ and $t = 59.7$ corresponding to the contours whose color coding can be accordingly read, and, the energy and Hamiltonian spectra (middle, lower). The period is normalized from 2π to 2. The arrows are added to highlight the propagation of the apparently solitonic longons.

As illustrated in the left frame of Fig. 3 for the u -contour/carpet, the “universality” of the scenario of orbits attracted to the whiskered tori further extends to the above approximate u_0 , and the sharper longon interactions with such high $K = 85$: two head-on colliding solitonic longons, with their strengths roughly proportional to the respective speeds, travel among the much weaker (c.f., middle-upper frame) and less-ordered ones; the latter present “long” quasi-trajectories with relatively severe “phase/position shifts” (a terminology borrowed from classical soliton theory for analogue) upon interaction (like the ‘strange particles’ and ‘resonances’ in particle physics): another reason for the term “longon”. We may unify the emergence and decay of such ‘particles’ with the notion of chaotization and alternatively use terminologies such as ‘thermalization’, and any (statistically) stationary longulent state may also be termed ‘(statistical) equilibrium’. Viewing essentially all such oscillations as interacting solitonic longons may seem radical, yet it retains coherence and might find mathematical justification for such “nonintegrable” systems (see more remarks on “pseudo-integrability” suggested below).

Besides the conventional energy spectrum $E(|k|) := \langle |\hat{u}_k|^2 \rangle$, we may define

$$H(|k|) := \sum_p \langle \hat{u}_p \hat{u}_{k-p} \hat{u}_k^* + c. c. \rangle / 6 \quad (14)$$

with $\langle \bullet \rangle$ for time averaging. The energy transfer rate is $T(|k|) := \hat{i} \sum_p \langle \hat{u}_p \hat{u}_{k-p} \hat{u}_k^* - c. c. \rangle / 2$, showing some duality with $H(|k|)$. In GrBH absolute (statistical) equilibrium, $T = 0$ marks the balance of energy transfer, but H provides additional information of the structures.

For an appropriate sequence ω_O of the “hyperdispersive”-KdV (hKdV) dispersive functions $\omega(n)$ of the model $\hat{a}_n = -\hat{i}\omega(n)\hat{v}_n$ in Eq. (1), the decoupled GrBH sub-dynamics with well-prepared u_0 in can be approximated with $\omega_O(m) \rightarrow \infty$ for all $m \notin$ and $\omega_O(k) \rightarrow 0$ for all $k \in$. [For convenience of comparison, we abuse the notation by replacing hKdV variable symbol v with u .] The asymptotic GrBH sub-dynamics may be argued directly by the fact that the intra- and extra-Galerkin frequencies can not match to form a resonant triad with a large jump of $\omega(n)$ in the classical resonant wave theory: the extra-Galerkin modes, if set up initially, however, can have their own dynamics, not of the interest here though. For understanding some physics of dissipation, a choice of a in Eq. (1) in Ref.^[9] was the hyperviscous dissipation function $d_O = -\xi(k/k_G)^{2O}$ ($K < k_G < K + 1$) for integer $O \rightarrow \infty$, but more consistent with the current situation is the dispersive model such as the hKdV

$$\hat{a}_k = -\hat{i}\omega_O(k)\hat{v}_k; \omega_O = \begin{cases} \left(\frac{k}{k_G}\right)^{2O+1} & \forall k \notin \\ 0 & \forall k \in \end{cases} \quad (15)$$

without the necessity of forcing for (energy) balance, among other subtleties (we will come back to the persistence issue against forcing and damping after more discussions on the KAM tori). In the numerical computations^[17] with correspondingly the same lattice number $N = 512$ and initial data, $k_G = 85.5 = K + 0.5$ and $O = 200$ are used in the hyper-dispersion Model (15). And, to avoid the slow change for $|k|$ near k_G^+ , $\omega_O(k)$ is empirically set to be $750 \operatorname{sgn}(k)(|k| - k_G)$ if $(|k|/k_G)^{401} < 1300$ (with the period normalized from 2π to 2 as in Fig. 3). We see in the middle-lower frame of Fig. 3 that E and H , respectively, are close and show the equipartition tendency at small wavenumbers ($|k| < 10$, say): persistence of the very-high-dimensional whiskered tori associated to the longlunt states are clearly indicated. Solitonic longon pulses approximate the Dirac delta function, thus the asymptotic large-scale energy equipartition; the nonlocal contribution to $H(|k|)$ at small $|k|$ from p is dominated by small- $|p|$ modes, thus also equipartitioned $H(|k|)$.

Note $\hat{i}(k/k_G)^{401} \hat{u}_k$ corresponds to a Hamiltonian component $(\partial_x^{200} u)^2 / (2k_G^{401})$ which however is minute, due to the smallness of \hat{u}_m for all $m \notin$: the GrBH \mathcal{H} is checked to be well preserved in the approximate model with tiny errors ($< 2\%$).

The hKdV structures shown in the right frame of Fig. 3 are also close to the GrBH ones (left frame). So, the results indicate the persistence, at least against hKdV(-like) models Eq. (15) with large- O (with closer longlunt for larger O verified — not shown) as the perturbation to Gr, of the GrBH whiskered tori/longlunt state, which is corroborated by other numerical results with different setups of various initial data, including the following zero-Hamiltonian ones.

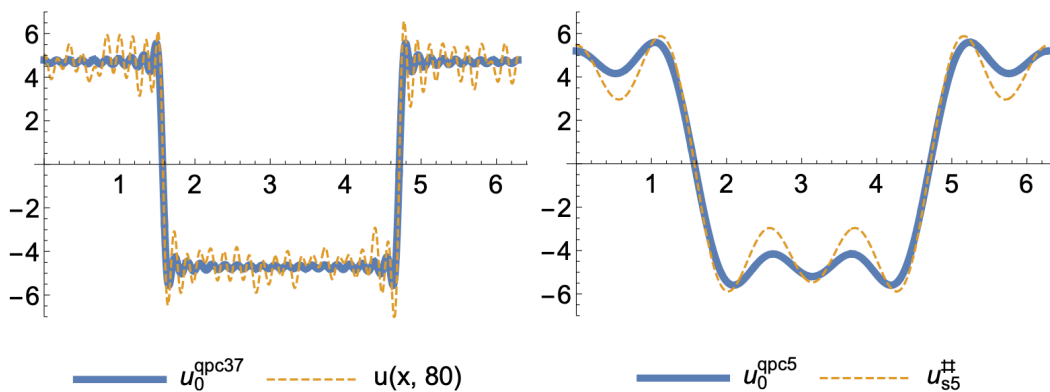


Figure 4. Well-developed $u(x, t)$ at a typical time $t = 80$ from u_0^{qpc37} with $K = 37$ (left), and, $u_{s5}^{\#}$ and u_0^{qpc5} (right); $Q = 3/2$ and $x_0 = -\pi/2$ for the QPC data.

Piecewise-constant $v_0 \sim \sum_k \frac{-2\hat{i}}{(2k+1)\pi} e^{\hat{i}(2k+1)x}$ is a weak solution to the BH equation, which suggests a quasi-piecewise-constant (QPC)

$$u_0^{qpcK} = Q \sum_{|2k+1| \leq K} \frac{-2\hat{i}}{(2k+1)\pi} e^{\hat{i}(2k+1)(x+x_0)}, \quad (16)$$

parameterized with Q . Fig. 4 (left panel) shows, among other selectively thermalized or random-like weaker oscillations in the well-developed u from u_0^{qpc37} , the persistent shock-antishock structure (as already in u_0^{qpc37}). The shock contributes a $E(|k|)$ -component $\propto k^{-2}$ as already explicitly given in the zero-Hamiltonian u_0^{qpcK} in Eq. (16).

2.4. On-torus invariants, quasi-periodic orbits, and persistence against some driving and damping

Further zero- λ solutions to the solitary-wave equation (4) are considered for insights associated to the a-posteriori KAM theorem^[15]: a stationary $u_{sK}^\#$ for $K = 37$ and slight deformation of it, responsible in the KAM fashion for the longulent $u(x, t)$ developed from u_0^{qpc37} in Fig. 4, should be close by, just as the comparison between u_0^{qpc5} and the stationary

$$u_{s5}^\# = 2(1 + \sqrt{3})\cos x + 2\cos(3x) + 2\cos(5x), \quad (17)$$

calculated through the ansatz similar to Eq. (16) with $K = 5$. For large K , $u_{sK}^\#$ s can be many, and it remains to identify the right one, including the possibility of other solutions with the replacement of the right-hand side of Eq. (4) by $\hat{i}\omega_K(k)\hat{u}_k^\#$. The longulence approximation (Fig. 3) with the linear dispersion (15), as a perturbation to , indicates similar persistence mechanism working around.

The above KAM claim can be strengthened and made more explicit, with the formulation resembling that of classical integrable systems (such as KdV in, e.g., Refs^{[10][11]}). The relevant tori carrying the quasi-periodic solutions “close” to $u^\#$ and the longulent solutions may be specified by a sub-set of invariants. With given invariants, we accordingly choose appropriate number of modes to be occupied with different frequencies, rationally-independent (incommensurate) or even Diophantine. For example, replacing the right-hand side of Eq. (4) by $-\hat{i}k(\lambda_0 + \lambda_1 k^2)\hat{u}_k^\#$, we can find various solutions which are quasi-periodic when λ_0 and λ_1 are rationally independent: this is realized by the variation principle

$$\delta(\mathcal{H} - \lambda_0 \mathcal{E}_0 - \lambda_\tau \mathcal{E}_\tau) / \delta u = 0, \quad (18)$$

with $\mathcal{E}_0 = \mathcal{E}$ and with $\tau = 1$ in $\mathcal{E}_\tau = \int_0^{2\pi} (\partial_x^\tau u)^2 / (4\pi) dx$, and such \mathcal{E}_τ is invariant along the specified torus (but, except for $\tau = 0$, in general should vary outside), because of the invariance of \mathcal{H} and \mathcal{E}_0 .

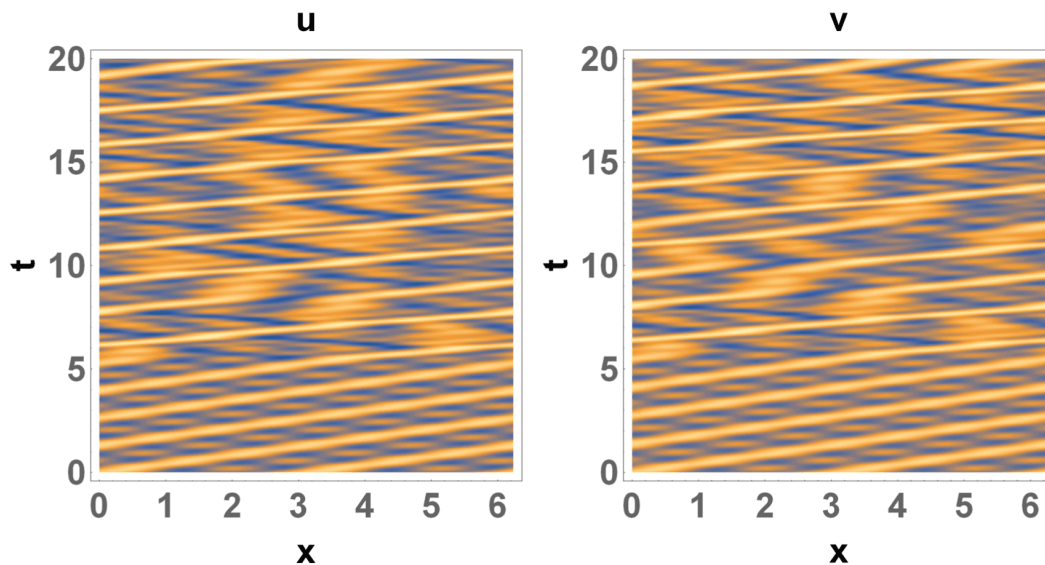


Figure 5. The u -contour with two-frequency parameterization for the GrBH (left) and the corresponding v -contour with forced-and-damped perturbation (right).

Longlentic patterns appearing closer to the exact solutions (compared to the one-phase travelling waves we have tested) can indeed be constructed with the help of additional on-torus invariants, as shown in Fig. 5 (left panel) of the case with $K = 4$, starting from the data of frequency vector with $\lambda_0 = \sqrt{6}/10$ and $\lambda_1 = \pi/10$.

With \mathfrak{I} invariants besides \mathcal{H} , including possibly other on-torus invariants than \mathcal{E}_τ , a \mathfrak{I} -torus can be similarly realized. And, some torus specified as such may correspond to the longlentic state such as that late-stage one in Fig. 3. That is, it might be expected that with the “right” additional on-torus invariant(s) a Gr-system becomes pseudo-integrable, in the sense of specifying precisely a longlentic state.

Finally, we are ready to discuss the persistence of the Gr-system longlentic states with respect to forcing and damping. As is well-documented, different choices of the forms of forcing and the (relative) strengths of forcing and damping can lead to various possibilities of the dynamical behaviors. Fine matching is typically needed to sustain the invariant tori, a nontrivial problem in

general. The remarkable physical example is the surface of magnetic flux (analogous to Hamiltonian mechanics^[12]) in controlled fusion where unmatched driving and dissipation can lead to the disruption. After various tests, we arrived at the model, following Eq. (1),

$$\partial_t v + v \partial_x v = a = \epsilon u(x, t) + D[v] \quad (19)$$

with small $\epsilon > 0$ and the simultaneous Gr-system u , and, D a suitable pseudo-differential of v resulting in a weak dissipative function such as $\hat{D} = d_O \hat{v}_k$ with the hyperviscous d_O mentioned before Eq. (15): this model appears to be universally working well, in the sense of making it easy to find the matched strengths of damping and forcing to have states arbitrarily close to the longlived ones of the corresponding Gr-systems studied here, including the GrBH case in Fig. 3 with large K ; although the original guiding intuition was that it should be more secured to work around the longlived u , both for the initial data and the “compensation” to bring v back to u (thus the simple driving ϵu), it turns out that the model actually works also well for more general initial data, as shown in Fig. 5. It suffices to showcase the example accompanying the above GrBH case associated to Eq. (18), leaving the more systematic analyses, including the computer-assisted proofs of other results, for another communication. For physical application in practice, one may first analytically or numerically find, or, (“machinely”) learn from the experimental data, the physically relevant tori associated to u and try to control the driving in such a way as ϵu for convenient construction of the states.

Fig. 5 presents a result, demonstrating persistence of the longlived (actually also the early dynamics), in the right panel from the same initial data for the GrBH u in the left panel. With the jump across k_G ($= 4.5$ here) being sharp and large enough, the details of the hyperviscous-type dissipation function appear nonessential. Fixing large enough O ($= 72$ with $\xi = 1$ in d_O here), several test runs are enough to find appropriately small ϵ by simply monitoring the energy levels at the beginning of each: here $\epsilon = 0.001$, around which small variations do not change the persistence result, with $|\int (v^2 - u^2) dx| / \int u^2 dx =: \delta < 1/20$, actually eventually $\delta < 1/60$ for large t .

3. Implications

The Galerkin regularization as an unusual pseudo-differential operator appears to make the rigorous proof more nontrivial; also challenging is to theoretically estimate the threshold for the breakup or stochasticity; see, e.g., Ref^[18] for successful cases. Rather than the mathematical details, the new physical implications, besides the above mentioned magnetic surface associated to transport barriers of fusion plasmas, to be emphasized in this end are the potential emergence of novel “particles”

(corresponding to the our longons) in the effective field theories of particle and condensed matter physics entailing truncations — be they fictitious or genuine — and the possible dependence on the details of forcing of the intermittency of turbulence at Reynolds numbers however large but not infinite: the latter, associated to the persistent “longulence” suggested here, is like our explanation for the non-Gaussian GrBH u and non-equipartition of $|\hat{u}_k|^2$ ^{[7][8]} with longon intermittency, and such structure-statistics aspects are also reminiscent of the change of Burgers turbulence by some specific forcing^[19].

In conclusion, the author thanks J. M. Hyman for motivating communications.

Footnotes

¹ See, e.g., recently, R. de la Llave and Y. Sire^[15]; and, A. P. Bustamante and R. de la Llave^[20].

² See L. Valvo and U. Locatelli^[21], successfully applied to create barriers to magnetic field line diffusion^[13].

References

1. ^{a, b}Olver PJ, Rosenau P. Tri-Hamiltonian duality between solitons and solitary-wave solutions having compact support. *Phys Rev E*. 53: 1900 (1996).
2. ^{a, b}Rosenau P. Nonlinear dispersion and compact structures. *Phys Rev Lett*. 73: 1737 (1994).
3. ^{a, b}Camassa R, Holm DD, Hyman JM. A New Integrable Shallow Water Equation. *Advances in Applied Mechanics*. 31: 1 (1994).
4. ^{a, b}Camassa R, Holm DD. An integrable shallow water equation with peaked solitons. *Phys Rev Lett*. 71: 1661 (1993).
5. ^{a, b}Rosenau P, Hyman JM. Compactons: Solitons with finite wavelength. *Phys Rev Lett*. 70: 564 (1993); and, for the Hamiltonian formulation, see Rosenau P, Zilburg A. Compactons. *J Phys A: Math Theor*. 51: 343001 (2018).
6. ^{a, b}Tadmor E. Convergence of Spectral Methods for Nonlinear Conservation Laws. *SIAM J Numer Anal*. 26: 30 (1989).
7. ^{a, b, c, d}Abramov R, Kovačič G, Majda AJ. Hamiltonian structure and statistically relevant conserved quantities for the truncated Burgers-Hopf equation. *Comm Pure Appl Math*. LVI: 0001 (2003).

8. ^{a, b, c}Abramov R, Majda AJ. *Discrete Approximations with Additional Conserved Quantities: Deterministic and Statistical Behavior. Methods and Applications of Analysis.* 10: 151 (2003).
9. ^{a, b}Frisch U, Kurien S, Pandit R, Pauls W, Ray SS, Wirth A, Zhu J-Z. *Hyperviscosity, Galerkin Truncation, and Bottlenecks in Turbulence. Phys Rev Lett.* 101: 144501 (2008).
10. ^{a, b, c, d}Dubrovin BA, Matveev VB, Novikov SP. *Non-Linear Equations of Korteweg-De Vries Type, Finite-Zone Linear Operators, and Abelian Varieties. Russ Math Surv.* 31: 59-146 (1976).
11. ^{a, b, c, d}Lax P (with Hyman JM). *Almost Periodic Solutions of the KdV Equation. SIAM REVIEW.* 18: 351 (1976).
12. ^{a, b}Escande DF, Momo B. *Description of magnetic field lines without arcana. Rev Mod Plasma Phys.* 8: 16 (2024).
13. ^{a, b}Chandre C, Vittot M, Ciraolo G, Ghendrih Ph, Lima R. *Control of stochasticity in magnetic field lines. Nuclear Fusion.* 46: 33 (2005).
14. [^]Gardner CS. *Korteweg-de Vries Equation and Generalizations. IV. The Korteweg-de Vries Equation as a Hamiltonian System. J Math Phys.* 12: 1548 (1971).
15. ^{a, b, c, d}de la Llave R, Sire Y. *An A Posteriori KAM Theorem for Whiskered Tori in Hamiltonian Partial Differential Equations with Applications to some Ill-Posed Equations. Arch Rational Mech Anal.* 231: 971-1044 (2019).
16. [^]Bardos C, Tadmor E. *Stability and spectral convergence of Fourier method for nonlinear problems: on the shortcomings of the 2/3 de-aliasing method. Numer Math.* 129: 749 (2015).
17. [^]The large-0 stiffness is overcome by the "ETDRK4" scheme of S. M. Cox and P. C. Matthews [Exponential Time Differencing for Stiff Systems, *J. Comput. Phys.* 176, 430 (2002)].
18. [^]Escande DF, Mohamed-Benkadda MS, Doveil F. *Threshold of global stochasticity and universality in Hamiltonian systems. Physics Letters A.* 101: 309 (1984).
19. [^]Chekhlov A, Yakhot V. *Kolmogorov turbulence in a random-force-driven Burgers equation. Phys Rev E.* 51: R2739 (1995).
20. [^]Bustamante AP, de la Llave R. *A Simple Proof of Gevrey Estimates for Expansions of Quasi-Periodic Orbits: Dissipative Models and Lower-Dimensional Tori. Regul Chaot Dyn.* 28: 707-730 (2023).
21. [^]Valvo L, Locatelli U. *Hamiltonian control of magnetic field lines: Computer assisted results proving the existence of KAM barriers. Journal of Computational Dynamics.* 9: 505 (2022).

Declarations

Funding: No specific funding was received for this work.

Potential competing interests: No potential competing interests to declare.